REMARKS

Applicants request reconsideration of the rejection in view of these remarks. Claims 1-15 and 18-29 are pending. Claims 24-29 are withdrawn from consideration.

The rejection under 35 U.S.C. §103(a)

Applicants maintain their traversal of the rejection of claims 1-3, 5-11, 13, and 16-23 as being obvious over Kidoguchi '586, the rejection of claim 4 as being obvious over Kidoguchi '586 in view of Koike '770, the rejection of claims 12 and 14 as being obvious over Kidoguchi '586 in view of Sarayama '663, and the rejection of claim 15 as being obvious over Kidoguchi '586 in view of Sarayama '663 and D'Evelyn '434. Particularly, Applicants traverse the rejection's assertion that the formation of a Group III nitride layer having a cycle of gaps of at least 100 μm is merely discovering an optimum value of a result effective variable that involves only routine skill in the art.

Applicants have explained in the previous amendment and response mailed April 11, 2008 that forming a seed crystal substrate with a cycle of gaps of at least 100 μm was not thought to be possible at the time of the invention, let alone involving "only routine skill in the art to optimize a value."

Applicants further submit two research papers to provide evidence and scientific reasoning that forming Group III nitride crystals on a Group III nitride layer having a cycle of gaps of at least 100 μm could not have been considered a problem of mere optimization and was not within the purview of one of ordinary skill in the art at the time of the present invention. One paper, Ishibashi et al., Jpn. J. Appl. Phys. Vol.42 (2003) pp. L 1248-1251 explains the problems of tilt and distortion when growing GaN crystals on a seed substrate having gaps using a vapor growth method. This is shown in, for example, Figures 2(a) to 2(c) of Ishibashi and especially the explanatory diagrams below the figures. Kidoguchi '586 as stated in column 17, lines 34-37 discloses a cycle of gaps of 18 μm. Ishibashi teaches that the problems of tilt and distortion at this cycle of gaps of 18 μm, the same periodicity of Kidoguchi '586,

are very evident. Ishibashi, moreover, discloses that as the width of the wing over the spacing of gaps increases, i.e., as the cycle of gaps become larger, the tilt angle increases. As the tilt angle increases, the wings grown over the respective convex portions, i.e., the gaps, become resistant to coalescing with each other. Ishibashi establishes that growing crystals on a seed substrate with a gap spacing of 18 μm is extremely difficult and makes no mention of growing crystals at a larger gap cycle. Thus, at the time of the invention, not only do Kidoguchi '586 and Ishibashi not provide any suggestion or reason to try to grow crystals on a Group III nitride layer having a cycle of gaps of at least 100 μm, these references, especially Ishibashi, teach away from the claimed invention.

The second paper, Nataf et al., Journal of Crystal Growth 192 (1998) pp. 73-78 also describes growing GaN layers on subtrates using vapor-phase epitaxy. When GaN crystals were grown on a seed substrate with masks (gaps) of 5 μm and windows (exposed portions of the GaN crystals) of 5 μm by a vapor growth method, plate-shaped GaN crystals were obtained, **provided the spacing region was not more than 10 μm**, *see* page 75, column l, and Figure 3a (emphasis added). Figure 3b explains that for a dielectric width larger than 10 μm, hexagonal holes appeared even for growth times as long as three hours, evidencing the difficulty for GaN bridges to completely link perpendicular to the stripes direction, *see* page 75, column l, and Figure 3b. Moreover, when a seed substrate with masks (gaps) of 100 μm and windows (exposed portions of the GaN crystals) of 10 μm were used, GaN grown from respective windows did not coalesce with each other at all; Figure 3c illustrates this phenomenon. Thus, Nataf et al. describe that there was not an expansion of a lateral plane (wing) leading to coalescence and plate-shaped GaN crystals were not obtained, *see* p. 75, left column, lines 1 to 6, and Figures 3b and 3c. In other words, Nataf et al. teach that growing Group III nitride crystals on a Group III nitride layer having a cycle of gaps of at least 100 μm could not be done.

These two references clearly demonstrate that, at the time of the invention, growing crystals on a seed substrate with a spacing of gaps of at least 100 μm was

extremely difficult, if not impossible, in light of the technical common knowledge at the time. A *prima facie* case of obviousness can be rebutted by showing that the art, in any material respect, teaches away from the claimed invention. Applicants assert that a teaching of a cycle of gaps of 5-20 μm, as in Kidoguchi '586, Ishibashi, and Nataf, teach away from a cycle of gaps of at least 100 μm, as required by claims 1, 12, and 18.

Further, none of Koike '770, Sarayama '663, and D'Evelyn '434, discloses, describes, suggests or provides a motivation for growing group III nitride crystals on a seed substrate with a cycle of gaps of at least 100 μm. Here, the rejection has not pointed to any teaching in the cited references, or provided any explanation based on scientific reasoning, that would support the conclusion that those skilled in the art would have considered it obvious to "optimize" the cycle of gaps to at least 100 μm, as required by claims 1, 12 and 18. On the contrary, Applicants have presented evidence that teaches growing group III nitride crystals on a seed substrate with a cycle of gaps of at least 100 μm could not be done. Ex parte Whalen II, BPAI (July 23, 2008) at 14.

Applicants assert that independent claims 1, 12 and 18 are not obvious and are allowable. Claims 2-11, 13-15 and 19-23 are also allowable at least by virtue of their dependence upon claims 1 and 18. Applicants do not concede the correctness of the rejection.

Application Number 10/758815
Response to the Office Action dated September 24, 2008

Should there by any remaining issues that could be easily resolved by telephone, the Examiner is invited to telephone Douglas P. Mueller at 612.455.3804.

Respectfully submitted,

HAMRE, SCHUMANN, MUELLER & LARSON, P.C.
P.O. Box 2902
Minneapolis, MN 55402-0902
(612) 455-3800

Dated: December 23, 2008

By: _____
Douglas P. Mueller
Reg. No. 30,300
DPM/KO/ad

Jpn. J. Appl. Phys. Vol. 42 (2003) pp. L 1248–L 1251
Part 2, No. 10B, 15 October 2003

Study on Deformations and Stress Distributions in Air-Bridged Lateral-Epitaxial-Grown GaN Films

Akihiko ISHIBASHI*, Gaku SUGAHARA, Yasutoshi KAWAGUCHI and Toshiya YOKOGAWA

Advanced Technology Research Laboratories, Matsushita Electric Industrial Co., Ltd., 3-1-1 Yagumo-Nakamachi, Moriguchi, Osaka 570-8501, Japan

(Received July 29, 2003; accepted August 25, 2003; published October 8, 2003)

Two-dimensional deformations and stress distributions in air-bridged lateral-epitaxial-grown GaN (ABLEG-GaN) films have been studied by atomic force microscopy (AFM), two-dimensional finite element method (FEM) analysis, and micro-Raman spectroscopy. The ABLEG-GaN wings slightly tilt, and the direction of the wing tilt changes when the wings coalesce with each other. After coalescence of the wings, the tilt angle decreases with increasing film thickness. By FEM analysis and Raman spectroscopy, it has been revealed that the deformation of the wings originates from the distributions of thermal stress due to large mismatch of the thermal expansion in the GaN seed layer and in the sapphire substrate. The wing deformation is suppressed with increasing film thickness, since the stress distribution becomes more uniform.
[DOI: 10.1143/JJAP.42.L1248]

KEYWORDS: GaN, air bridge, thermal stress, micro-Raman, finite element method

Group III nitrides are highly promising for applications in blue and ultraviolet optoelectronic devices and high-temperature, high-power transistors. Recent studies on the various selective area growth (SAG) techniques, such as epitaxial-lateral-overgrowth (ELO) and Pendeo-epitaxy of group III nitrides on sapphire and SiC substrates via metal-organic vapor phase epitaxy (MOVPE) have shown that they were extremely effective in reducing the threading dislocation (TD) density and markedly improved the performance of the devices, such as violet laser diodes.[1–5] However, there is a problem in that the ELO-GaN regions, hereafter called "wings", tilt crystallographically (about 1°). It is supposed that the crystallographic tilt of the wings originates from the stress at the interface between the wings and the mask, and the thermal stress due to the mismatch of thermal expansion between the GaN layer and a substrate.[6] The wing tilt induces the dislocations near the coalescence region of the wings.[7]

We have developed an advanced ELO structure, namely, "air-bridged lateral epitaxial grown (ABLEG)"-GaN,[8,9] which has no contact between the wing and the mask, as shown in Fig. 1. Since the wings in the ABLEG-GaN have no contact with the masks, there is no stress in the interface between the wings and the masks. Therefore, the wing tilt markedly decreases in the ABLEG-GaN and the TD densities are reduced not only in the wing region but near the coalescence boundary between the wings. The tilt angle is approximately 0.1°, and the TD density is 10^6 cm^{-2} in the ABLEG-GaN wings. It is supposed that the wing tilt is due to the thermal stress generated between the GaN-seed layer and the sapphire substrate, not the stress in the interface between the wings and masks. The local stress analysis of the ELO-GaN deposited on SiO_2 masks was reported.[10] Though the strain and crystallographic tilt in uncoalesced GaN layers grown by maskless Pendeo-epitaxy have been studied,[11] there are few reports on the quantitative analysis of the deformation induced from the thermal stress in the coalesced ELO-GaN.

In this work, we have studied the wing deformations resulting from the thermal stress distributions in the ABLEG-GaN films on the sapphire substrates by atomic force microscopy (AFM), the finite element method (FEM) based on the two-dimensional orthotropic linear elastic theory, and micro-Raman spectroscopy. It was found that the calculation results on the deformation of the wings in the ABLEG-GaN are in good agreement with the experimental results.

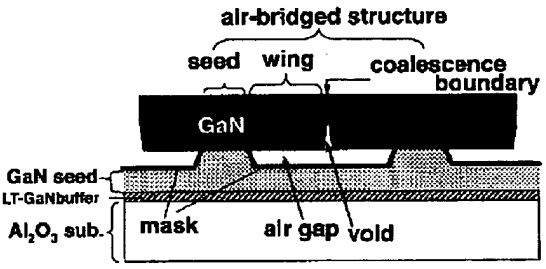

Fig. 1. Schematic cross-sectional diagram of the ABLEG-GaN.

Figure 1 shows the schematic cross-sectional diagram of the ABLEG-GaN. A 1.2-μm-thick (0001) GaN layer is grown on the (0001) sapphire substrate with a 20-nm-thick low-temperature (LT) GaN buffer layer by low-pressure MOVPE. The GaN film is grooved to form ridge stripes along the $<1\bar{1}00>_{GaN}$ direction. The width and the period of the ridge stripes are 3 and 15 μm, respectively. Next, the 10-nm-thick silicon nitride mask is deposited on the grooved GaN film. After that, only the silicon nitride mask on the top of the ridge stripes is removed, and the silicon nitride mask on the sidewalls and bottoms of the grooved GaN film is left. The ABLEG is performed on the exposed (0001) GaN top surface which is a seed crystal for regrowth. When the coalescence of the wings occurs, the air-bridged structure is constructed. A smooth surface is obtained not only in the wing region, but in the vicinity of the coalescence boundary. The tapered voids are formed below the coalescence boundary surfaces. Some details of the growth and process conditions are reported in refs. 8 and 9.

The surface conditions and deformations of the wings are characterized by AFM. The AFM is carried out in the tapping mode using a Digital Instruments Dimension 3100 scanning probe microscope. The crystallographic tilt is characterized by X-ray diffraction (XRD) measurements.

*E-mail address: isibasi.akihiko@jp.panasonic.com

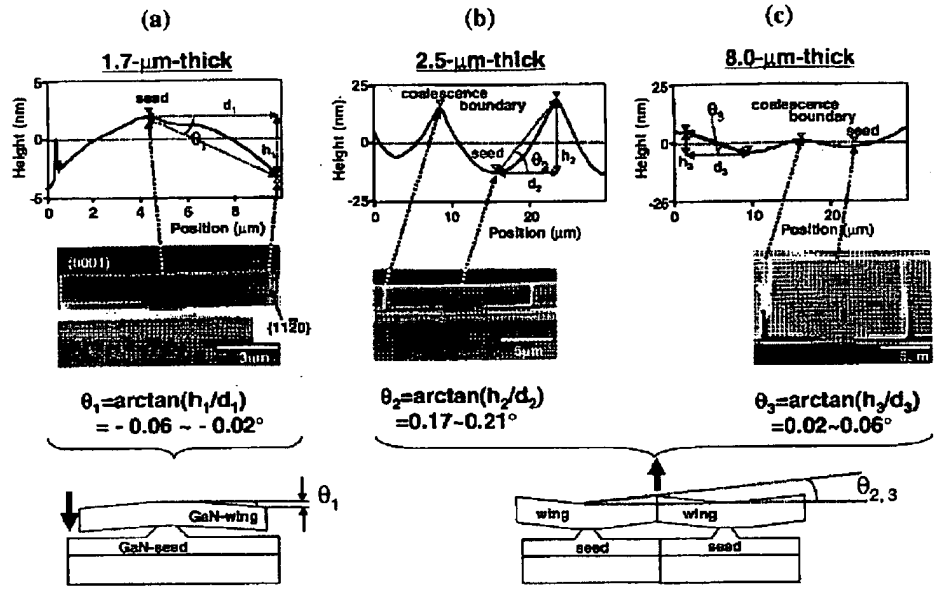

Fig. 2. Cross-sectional SEM images and AFM profiles of the surfaces in the ABLEG-GaN, whose wings are uncoalesced (a), and coalesced (b)-(c), respectively.

The wing deformations resulting from the thermal stress distributions in the ABLEG-GaN films on the sapphire substrates have been simulated by FEM based on the two-dimensional orthotropic linear elastic theory.[12] We assumed that the thermal stress is only due to the mismatch of thermal expansion coefficient (α) between GaN and the sapphire substrate during the cooling process after epitaxial growth. The temperature is changed from 1000°C to 25°C during the cooling process. The components of the elasticity theory are the mismatch of α between GaN and the substrate and a set of moduli of elasticity. We used the moduli of elasticity for GaN and the sapphire in refs. 13–15.

The stress distributions are characterized by a frequency shift in the micro-Raman spectroscopy measurements. In these measurements, light from the 514.5 nm line of an Ar^+-ion laser is focused on the $(1\bar{1}00)_{GaN}$ surface of the cleaved ABLEG-GaN at room temperature. The diameter of the focused area is below 1 μm. In this backscattering geometry, the A_1(TO), E_1 (TO), and E_2 modes are allowed on the basis of the selection rules.

Figure 2 shows the cross-sectional scanning electron microscopy (SEM) image and the AFM profiles of the surface in the ABLEG-GaN, whose wings are uncoalesced (a), and coalesced (b)-(c), respectively. In the case of the uncoalesced wing, the height of the wing edge is lower than that of the center of the wing. The tilt angle θ_1, which is defined as arctan (h_1/d_1) in Fig. 2 (a), is about -0.06° ~ -0.02°, where the minus sign denotes the $<000\bar{1}>_{GaN}$ direction. In case of the coalesced wings, the coalescence boundary is higher than that in the seed region. The tilt angle θ_2 is 0.17° ~ 0.21° for the film thickness of 2.5 μm, and θ_3 is 0.02° ~ 0.06° for the film thickness of 8.0 μm. Therefore, the tilt angle decreases with increasing film thickness.

In order to determine the origin of the wing deformation,

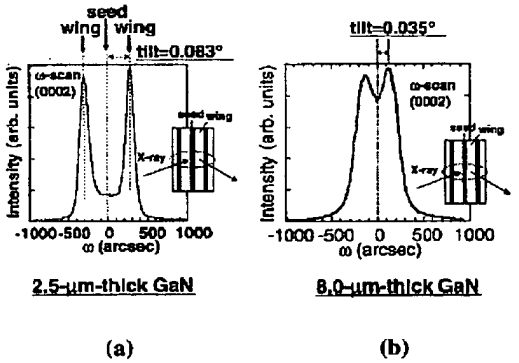

Fig. 3. X-ray rocking curves (XRCs) of the (0002) ω scan for $\varphi = 0°$, where φ is the angle between the rotation axis of the ω scan and the stripe direction.

XRD measurements are performed, where the direction of the incident X-ray beam is perpendicular to the stripe. Figure 3 shows X-ray rocking curves (XRCs) of the (0002) ω scan for $\varphi = 0°$, where the azimuth φ is the angle between the rotation axis in the ω scan and the stripe direction. Three diffraction peaks are observed, that is two satellite peaks and one small peak at the center between the satellite peaks. The two satellite peaks are located ±0.083° (±0.035°) from the center peak for the 2.5-μm (8.0-μm)-thick GaN film. The tilt angle decreases with increasing film thickness. For $\varphi = 90°$, only the single peak is observed for any thickness. Therefore, the wing deformation originates from the crystallographic tilt of the c-axis perpendicular to the stripe.

Since the thermal expansion coefficient of GaN is smaller than that of sapphire, the compressive stress is produced in

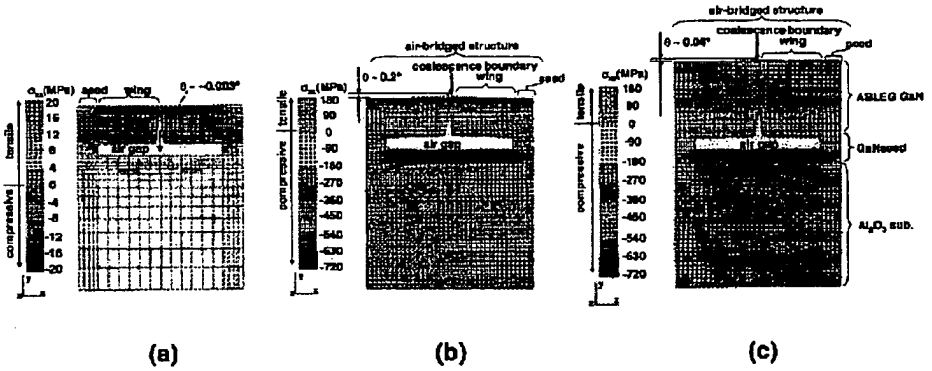

Fig. 4. Calculated thermal stress distributions along the x-axis (σ_{xx}) before coalescence of the wings (a), and after coalescence of the wings (b)-(c), respectively.

the epitaxial GaN layer on the sapphire substrate when the sample is cooled from the growth temperature to the room temperature. The stress distribution produces elastic deformation of the GaN layer. In ABLEG-GaN, since the wings are located above the air gap, the elastic deformation can easily occur. We have simulated the elastic deformation by FEM.

The calculated thermal stress distributions along the x-axis (σ_{xx}) are shown, for the 3-μm-thick wing (uncoalesced) in Fig. 4 (a), the 3-μm-thick wing (coalesced) in Fig. 4 (b), and the 6-μm-thick wing (coalesced) in Fig. 4 (c). The shape is modified, on the condition that the nodal displacement along the y direction (DY) is multiplied by 16, in order to make it easy to understand the deformation. Before coalescence, the compressive stress (about 300 MPa) exists in the GaN seed layer due to the large mismatch of the thermal expansion coefficient. In the seed region of ABLEG-GaN, a large compressive stress exists at the bottom, while a small tensile stress exists near the surface. In the wing region, the stress is nearly free. As a result, the wing bends slightly downwards. Just after coalescence, the compressive stress (about 300 MPa) exists in the GaN seed layer, similar to that before coalescence. In the wing region, a large compressive stress concentrates at the coalescence boundary region and the tensile stress exists at the bottom surface of the wings. As a result, the wings bend and the coalescence boundary becomes higher than the seed region. The tilt angle of the wings, for the thickness of 3 μm, is about 0.2°, which is in good agreement with the experimental result. For the thickness of 6 μm, a larger compressive stress concentrates at the coalescence boundary region compared with other regions. However, the stress becomes more uniformly distributed along the x-direction, compared with that for the thickness of 3 μm.

It is supposed that the wing deformations originate from the stress distributions and the relaxation in the air gap, the void, and the surface. There is highly compressive stress in the GaN seed layer, which brings about compressive stress in the wings. Since the compressive stress can relax in the x-direction on both sides of the void, the wings can extend in the x-direction. Therefore, the compressive stress along the x-direction is cancelled on both sides of the void. This result causes highly compressive stresses along the x-direction just above the void. As a result, the wings expand in the y-direction, and the deformation of the wings occurs. Therefore, it is found that the wing deformation in the vicinity of the coalescence boundary is due to the stress relaxation near the tapered void.

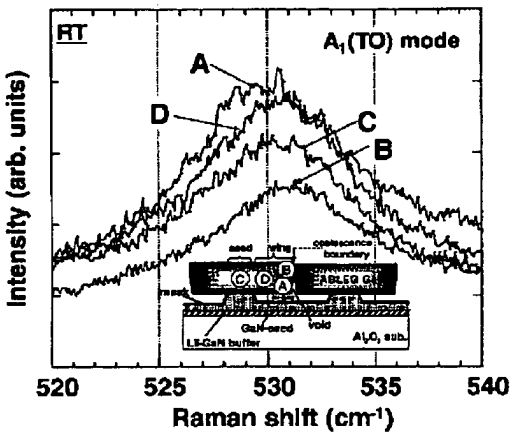

Fig. 5. A_1(TO)-mode micro-Raman spectra for various spots in the cleaved $(1\bar{1}00)_{GaN}$ surface of ABLEG-GaN.

The stress distributions can be characterized by the frequency shift in the micro-Raman spectroscopy measurements.[16,17] Figure 5 shows the A_1(TO)-mode micro-Raman spectra for various spots in the cleaved $(1\bar{1}00)_{GaN}$ surface in the 6-μm-thick ABLEG-GaN. The Raman peak wave number depends on the measurement spot. The E_2 mode lines showed almost the same frequency shift as the A_1(TO)-mode. The highest wave number was observed at the coalescence boundary above the void (spot B), while the lowest was observed at the bottom of the wing near the void (spot A). In the seed region (spot C) and the midwing region (spot D), the peak wave number was observed between spots A and B. The frequency shift in the micro-Raman spectroscopy measurements shows the existence of the stress distribution in the ABLEG-GaN films. The estimated stress difference between spots A and B is about 200 MPa.[16] These results are in good agreement with the FEM calculation results.

In summary, two-dimensional deformations and stress distributions in ABLEG-GaN films have been studied by AFM, two-dimensional FEM analysis, and micro-Raman spectroscopy. The ABLEG-GaN wings slightly tilt, and the direction of the wing tilt changes when the wings coalesce with each other. After coalescence of the wings, the tilt angle decreases with increase of the film thickness. By FEM analysis and Raman spectroscopy, it has been revealed that the deformation of the wings originates from the distributions of thermal stress due to large mismatch of the thermal expansion in the GaN seed layer and in the substrate. The wing deformation decreases with increasing film thickness, since the stress distribution becomes more uniform.

The author wishes to thank Dr. K. Eda for his encouragement, and Drs. I. Kidoguchi and Y. Hasegawa for useful discussion. The author wishes to acknowledge technical support from H. Morita and E. Mizoguchi.

1) T. Nishinaga, T. Nakano and S. Zhand: Jpn. J. Appl. Phys. **27** (1988) L964.
2) A. Usui, H. Sunakawa, A. Sakai and A. A. Yamaguchi: Jpn. J. Appl. Phys. **36** (1997) L899.
3) T. S. Zheleva, O. H. Nam, M. D. Bremser and R. F. Davis: Appl. Phys. Lett. **71** (1997) 2472.
4) S. Nakamura, M. Senoh, S. Nagahama, N. Iwasa, T. Matsushita and T. Mukai: MRS Internet J. Nitride Semicond. Res. **4S1** (1999) G1.1.
5) Y. Honda, Y. Iyechika, T. Maeda, H. Miyake and K. Hiramatsu: Jpn. J. Appl. Phys. **40** (2001) L309.
6) S. Tomiya, K. Funato, T. Asatsuma, T. Hino, S. Kijima, S. Asano and M. Ikeda: Appl. Phys. Lett. **77** (2000) 636.
7) A. Sakai, H. Sunakawa and A. Usui: Appl. Phys. Lett. **73** (1998) 481.
8) I. Kidoguchi, A. Ishibashi, G. Sugahara and Y. Ban: Appl. Phys. Lett. **76** (2000) 3768.
9) A. Ishibashi, I. Kidoguchi, G. Sugahara and Y. Ban: J. Cryst. Growth **221** (2000) 338.
10) Q. Liu, A. Hoffmann, A. Kaschner, C. Thomsen, J. Christen, P. Veit and R. Clos: Jpn. J. Appl. Phys. **39** (2000) L958.
11) S. Einfeldt, A. M. Roskowski, E. A. Preble and R. F. Davis: Appl. Phys. Lett. **80** (2002) 953.
12) *SAMCEF 8.1 User's Manuals* (Samtech, Belgium and Surigiken Co. Ltd., Tokyo, 2000)
13) T. Detchprohm, K. Hiramatsu, K. Itoh and I. Akasaki: Jpn. J. Appl. Phys. **31** (1992) L1454.
14) V. A. Savastenko and A. U. Sheleg: Phys. Status Solidi A **48** (1978) K135.
15) H. P. Maruska and J. J. Tietjen: Appl. Phys. Lett. **15** (1969) 327.
16) T. Kozawa, T. Kachi, H. Kano, H. Nagase, N. Koide and K. Manabe: J. Appl. Phys. **77** (1995) 4389.
17) H. Siegle, P. Thurian, L. Eckey, A. Hoffmann, C. Thomsen, B. K. Meyer, H. Amano, I. Akasaki, T. Detchprohm and K. Hiramatsu: Appl. Phys. Lett. **68** (1996) 1265.

ELSEVIER

Journal of Crystal Growth 192 (1998) 73–78

JOURNAL OF CRYSTAL GROWTH

Lateral overgrowth of high quality GaN layers on GaN/Al_2O_3 patterned substrates by halide vapour-phase epitaxy

G. Nataf*, B. Beaumont, A. Bouillé, S. Haffouz, M. Vaille, P. Gibart

Centre de Recherche sur l'Hétéroépitaxie et ses Applications (CRHEA-CNRS), Sophia Antipolis, 06560-Valbonne, France

Received 20 February 1998

Abstract

The growth of GaN thick layers by halide vapour-phase epitaxy (HVPE) on metalorganic vapour-phase epitaxy (MOVPE)-GaN/Al_2O_3 substrates is reported. In a first step, we have shown that lateral overgrowth was enhanced following preferential crystallographic directions. Double crystal X-ray diffraction (DCXRD) assessment in ω scan showed full-width at half-maximum (FWHM) as small as 50 arcsec. On the way towards the realisation of self-supported GaN substrates, the present study was extended to epitaxial lateral overgrowth (ELOG) on large surface GaN/Al_2O_3 patterned substrates to achieve coalescence. Structural, electrical and optical characterisation of such layers was performed, underlining the promising quality of these materials.

PACS: 81.05.Ea; 81.15.Gh

Keywords: Selective epitaxy; Lateral overgrowth; Growth anisotropy; MOVPE; HVPE

1. Introduction

GaN and III–V related compounds are essential materials for devices operating in the green to UV region of the spectrum. Blue LD's and green to blue LED's have already been realised by the MOVPE technique [1–7]. Presently, due to great difficulties in growing stable bulk GaN single crystals, the major challenge is to overcome the lack of an appropriate substrate. For example, Unipress in Poland has grown GaN from gallium melts [8,9]. However, the size of GaN single crystals produced by this technique is only a few square millimetres, although their structural quality is very good.

Among the alternative substrates, the most widely used is Al_2O_3, although SiC, ZnO, $MgAl_2O_4$... have also been tried. However, all of these crystals present large lattice parameters and thermal coefficient differences with those of GaN leading to highly strained and dislocated layers. Therefore, the important defect densities always observed in GaN layers, degrade tremendously the quality of GaN based devices. During the last year, several groups

* Corresponding author. Fax: +33 4 9395 8361; e-mail: gn@crhea.cnrs.fr.

0022-0248/98/$19.00
PII: S0022-0248(98)00413-8

have demonstrated the effectiveness of localised epitaxial lateral overgrowth (ELOG) on patterned substrates to reduce this defect density [10,11]. Most of the early works devoted to the elaboration of GaN layers on sapphire substrates used the HVPE process. More recently, HVPE which allows high growth rates for good quality materials was reported to supply thick GaN films on Al_2O_3 substrates [12,13]. In this work, HVPE has been carried out directly, to produce ELOG layers up to coalescence.

2. Experimental procedure

The growth of GaN was carried out in a home-made HVPE system with a horizontal reactor. A HCl + N_2 mixture (purity 99.999%) was made to react in a silica boat with gallium (purity 99.99999%) at 1000°C, then GaCl was introduced with NH_3 in the growth zone to form GaN. N_2 was used as the carrier gas. HCl, NH_3 and N_2 were purified by means of getters. The heating phase was carried out under NH_3 flow and the growth was started as soon as the substrate temperature reached 1050°C. GaN layer thickness ranging from 30 to 150 μm were obtained at growth rates up to 30 μm/h. Fig. 1 shows a schematic drawing of the system.

The substrates used here were MOVPE-GaN layers grown on (0 0 0 1)sapphire with a thin GaN low-temperature buffer layer. Growth conditions for these layers are published elsewhere [14]. GaN layers were coated with a very thin silicon nitride film (~2 nm) in the same MOVPE run and then the mask openings were defined by photolithography and ECR etching.

In a first approach, two kinds of masks were designed to assess the main growth parameters. The first one was star-shaped with line openings 5 μm wide and 350 μm long oriented with a 5° angular increment. In one corner of this feature, a rectangular field of hexagonal holes (5 μm diameter separated by 10 μm) was also implemented. The second one was made of a line array with 5 or 10 μm openings and a periodicity ranging between 5 and 100 μm. The stripe's length was 2 mm.

3. Growth results

Several growths with 0.5–3 h duration were performed on each of these patterned GaN/Al_2O_3 substrates. Fig. 2a shows a HVPE-GaN layer grown on star-patterned openings. As a result of growth on the star-patterned openings, an obvious trend towards lateral extension for stripes following the directions $\langle 0\,\bar{1}\,1\,0\rangle$ can be observed, showing that the lateral on vertical growth rate ratio is then maximum (Fig. 2a). As pointed out by other authors [15], the ends of the lines tend towards a pyramidal form revealing the slow growing facets $\{1\,\bar{1}\,0\,1\}$ (Fig. 2b). It must be pointed out that the amount of lateral overgrowth is closely dependent upon the concentration of atomic nitrogen in the vapour phase, consequently it is magnified with high temperature and high ammonia flows as

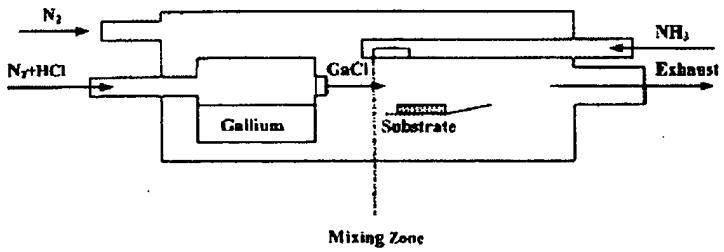

Fig. 1. Schematic diagram of the HVPE reactor. The counter-flow NH_3 line allows to separate the mixing zone from that of GaCl introduction.

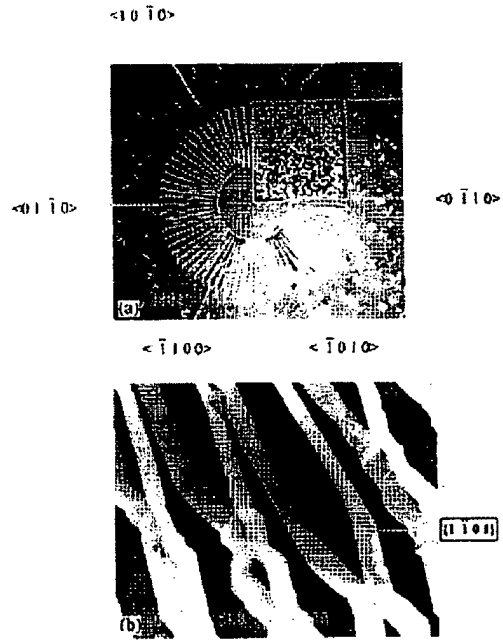

Fig. 2. SEM micrographs of a GaN layer grown on a star-patterned substrate. (a) When the stripes follow the directions $\langle 0\,\bar{1}\,1\,0\rangle$. LOG is enhanced; (b) detail of triangular termination of growth following a stripe along $\langle 0\,\bar{1}\,1\,0\rangle$.

reported by Kapolnek et al. for MOVPE-grown GaN [10].

For runs performed on stripe-patterned substrates, coalescence was achieved for stripes following $\langle 0\,\bar{1}\,1\,0\rangle$ directions, when window openings were 5 or 10 μm wide, and, provided the spacing region was not more than 10 μm. Fig. 3a represents a SEM cross-section micrograph of a continuous GaN film grown on a stripe-patterned region. In the region near the interface, the voids indicate the location where the coalescence took place. Emerging from each void, a chimney goes vertically up to the surface. For dielectric width larger than 10 μm, hexagonal holes appeared even for growth times as long as 3 h showing the difficulty for GaN bridges to completely link perpendicular to the stripes direction (Fig. 3b). The mechanism involved in such lateral overgrowth appears quite different from the one observed for other III–V semiconductors as GaAs [16]. Here there is not an expansion of a lateral plane leading to coalescence, but rather localised nucleations throwing separate lateral bridges between two stripes, followed by an extension along the stripes to form a continuous film (Fig. 3c).

Concerning HVPE-GaN growths on hexagonal holes, two observations arose. First, at the early 30 min of the growth, well-shaped hexagonal prisms were formed (Fig. 4a) whose facets belong to the $\{1\,\bar{1}\,0\,1\}$ family as already seen by the MOVPE technique [17]. For a longer growth time, bridges appeared linking the different pyramids and then coalescence could take place (Fig. 4b). The result was a flat homogeneous film with remaining holes. Preliminary assessment by DCXRD of such small areas of GaN overgrown layers showed a FWHM of 50 arcsec in ω scan.

4. HVPE lateral overgrown GaN

The next step towards the achievement of self-supported substrates was the realisation of GaN lateral overgrown thick layers on larger surfaces. For this purpose, two other masks were designed to allow large area patterns, consisting either of hexagonal dots or of parallel stripes. At present, only the first one was tried. Using previous growth conditions, it was possible to realise continuous laterally overgrown thick GaN layers (up to 150 μm) presenting a flat surface. However, although globally very smooth, the surface presented numerous hexagonal holes with a depth up to 50 μm, depending on the way the linking between neighbouring hexagonal pyramids took place.

5. Structural assessment

DCXRD measurements carried out on lateral overgrown HVPE-GaN layers on large surface hexagonal patterned substrates showed FWHM in ω scan ranging between 300 and 450 arcsec. These results are clearly poor as compared to the 50 arcsec previously reported in this paper for ELOG on a very small area. Recently, Sakai et al. [17] showed, by TEM observations on selectively grown

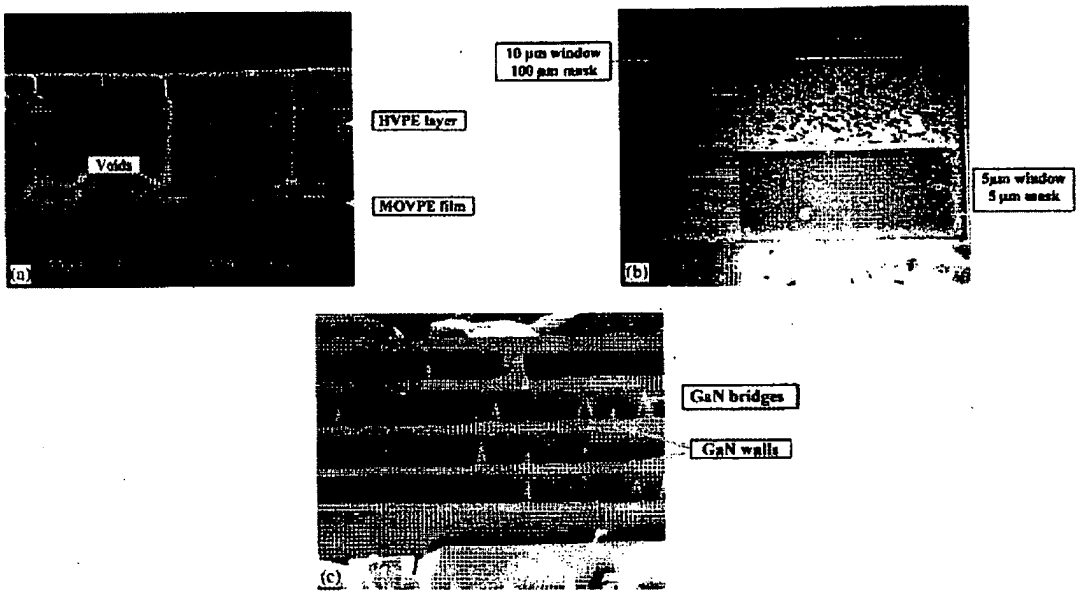

Fig. 3. SEM micrographs of GaN grown on a stripe-patterned substrate. (a) The cross section shows voids terminated by a chimney at the interface between the MOVPE layer and the LOG-HVPE layer; (b) surface view evidences that complete coalescence is achieved on stripes with lower periodicity (5 μm mask × 5 μm window at the right bottom); (c) on stripes with higher periodicity (100 μm mask × 10 μm window) bridges showing the LOG mechanism are seen.

GaN by HVPE on MOVPE layers, that most of the threading dislocations vertically aligned in the MOVPE-grown layer, propagated laterally around the SiO_2 mask in the HVPE film, before the film thickness reached about 5 μm. Hence, this enlargement of FWHM in the case of large area ELOG GaN, could be attributed to the sample bending due to the important residual stress existing between the GaN layer and the Al_2O_3 substrate rather than a degradation of the defect density. Consequently, we need to check the defect density observed on such a layer by TEM direct observation. This study will be carried out in the near future.

6. Physical characterisation

Hall–Van der Pauw assessment performed on ELOG-GaN showed room temperature mobility up to 210 $cm^2/V\,s$ for electron concentrations as low as $3 \times 10^{17}\ cm^{-3}$.

Low-temperature (10 K) photoluminescence spectrum (Fig. 5), is dominated by near band edge excitonic transitions involving free exciton A (3.481 eV), a donor bound exciton I_2 (3.474 eV) and acceptor bound exciton I_1 (3.462 eV). In the 3.27 eV range, donor–acceptor pairs recombinations (D^0A^0) were observed involving the usual donors and acceptors of GaN. According to the literature, these numerical values show that this GaN layer is fully relaxed. Closer examination of this spectrum showed that the intensity ratio of band edge to acceptor related transitions got close to two orders of magnitude. This is in agreement with the low residual impurity level measured by the Hall effect. According to previous studies performed on HVPE-GaN layers on sapphire, there was no yellow band detected in these ELOG-GaN samples.

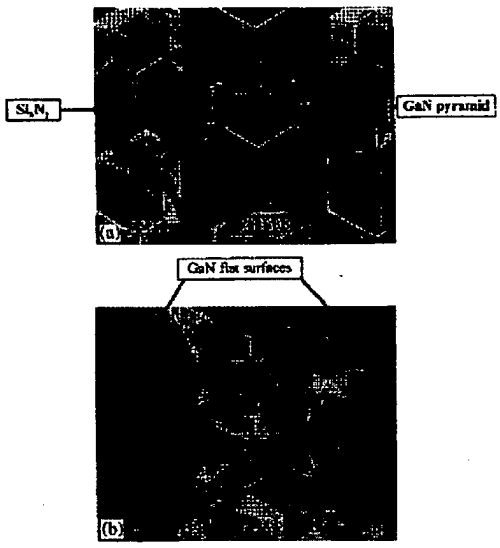

Fig. 4. SEM micrographs of GaN grown on an hexagonal holes field. (a) After 30 mn growth, well shaped pyramids are formed; (b) later, coalescence takes place leading to flat surfaces separated by holes or valleys.

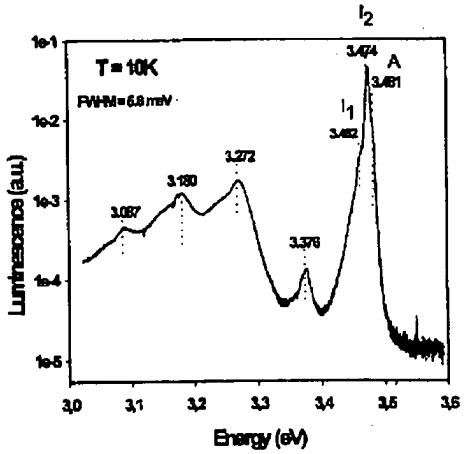

Fig. 5. Low-temperature photoluminescence spectrum. Near band edge feature shows I_2 (3.4746 eV), A (3.4809 eV) and I_1 (3.4620 eV) lines.

7. Discussion

Thick GaN layers overgrown by HVPE on patterned MOVPE-GaN/Al_2O_3 substrates present structural and physical properties of high quality. The total reduction in the density of defects has presently to be demonstrated and further progress is still expected but it is clear that large area ELOG represents an important step towards self-supported GaN substrates.

Acknowledgements

This work was supported by an ESPRIT-LTR contract from the European Union, LAQUANI N°20968. The authors wish to thank MM J.C. Guillaume, M. Passerel, Dr. M. Leroux and Dr. O. Parillaud for helpful advice.

References

[1] S. Nakamura, G. Fasol, The Blue Laser, Springer, Berlin, 1997.
[2] R.P. Vaudo, I.D. Goepfert, T.D. Moustakas, D.M. Beyea, T.J. Frey, K. Meehan, J. Appl. Phys. 79 (5) (1996) 2779.
[3] T.J. Schmidt, X.H. Yang, W. Shan, J.J. Song, W. Kim, Ö. Aktas, A. Botchkarev, H. Morkoç, Appl. Phys. Lett. 68 (13) (1996) 1820.
[4] S. Kurai, Y. Naoi, T. Abe, S. Ohmi, S. Sakai, Jpn. J. Appl. Phys. 35 (1996) L77.
[5] P.A. Maki, R.J. Molnar, R.L. Aggarwal, Z.L. Liau, I. Melngailis, Mater. Res. Soc. Symp. Proc. 395 (1996) 919.
[6] B. Beaumont, P. Gibart, M. Leroux, E. Calleja, E. Munoz, E-MRS 97, Strasbourg, 1997, Mater. Sci. Eng., to be published.
[7] B. Beaumont, F. Calle, S. Haffouz, E. Monroy, M. Leroux, E. Calleja, P. Lorenzini, E. Munoz, P. Gibart, Proc. Int. Conf. On Silicon Carbide, III-Nitrides and Related Materials, Stockholm, to be published.
[8] S. Porowski, J. Crystal Growth 166 (1996) 583.
[9] T. Suski, P. Perlin, M. Leszczynski, H. Teisseyre, I. Grzegory, J. Jun, M. Bockowski, S. Porowski, K. Pakula, A. Wysmolek, J.M. Baranowski, Mater. Res. Soc. Symp. Proc. 395 (1996) 15.
[10] D. Kapolnek, S. Keller, R. Vetury, R.D. Underwood, P. Kozodoy, S.P. Den Baars, U.K. Mishra, Appl. Phys. Lett. 71 (9) (1997) 1204.
[11] X. Li, A.M. Jones, S.D. Roh, D.A. Turnbull, S.G. Bishop, J.J. Coleman, J. Electron. Mater. 26 (3) (1996) 306.

[12] K. Naniwae, S. Itoh, H. Amano, K. Itoh, K. Hiramatsu, I. Akasaki, J. Crystal Growth 99 (1990) 381.
[13] T. Detchprohm, K. Hiramatsu, H. Amano, I. Akasaki, Appl. Phys. Lett. 61 (22) (1992) 2688.
[14] B. Beaumont, M. Vaille, T. Boufaden, B. El Jani, P. Gibart, J. Crystal Growth 170 (1997) 316.
[15] Ok-Hyun Nam, M.D. Bremser, B.L. Ward, R.J. Nemanich, R.F. Davis, Jpn. J. Appl. Phys. 36 (1997) L 532.
[16] G. Nataf, M. Leroux, S.M. Laügt, P. Gibart, J. Crystal Growth 165 (1990) 1.
[17] A. Sakai, H. Sunakawa, A. Usui, Appl. Phys. Lett. 71 (16) (1997) 2259.